Research Square

Preprints are preliminary reports that have not undergone peer review.
They should not be considered conclusive, used to inform clinical practice,
or referenced by the media as validated information.

Ganoderic acid A alleviates acute lung injury in mice by inhibiting ferroptosis via upregulating NLRP3

Zheng Luo
Shiqiaopu Sub-district Community Health Service Center
Xingqing Cheng
Shiqiaopu Sub-district Community Health Service Center
Guiyu Zhang
City University of Hong Kong
Jun Yan
Chongqing Western Frontier Biotechnology Research Institute
Yong Zhou
Chongqing Western Frontier Biotechnology Research Institute
Zailiang Yang
yangzailiang408000@cqu.edu.cn

Chongqing University of Chinese Medicine

Research Article

Keywords: Ganoderic acid A, Acute lung injury, Ferroptosis, Inflammation, NLRP3

Posted Date: June 26th, 2026

DOI: https://doi.org/10.21203/rs.3.rs-10011492/v1

License: This work is licensed under a Creative Commons Attribution 4.0 International License.
Read Full License

Additional Declarations: No competing interests reported.

Abstract

Acute lung injury (ALI) is a serious clinical condition that can lead to acute respiratory distress syndrome and even death. ferroptosis plays a significant role in its pathogenesis. Ganoderic acid A(GAA) is a key bioactive component of the traditional Chinese medicine Ganoderma lucidum. It exhibits anti-inflammatory, antioxidant, and anti-ferroptotic properties and can alleviate various inflammatory diseases, including acute pancreatitis, osteoarthritis. In this study, we found that GAA can inhibit LPS-induced inflammation and ferroptosis in human bronchial epithelial cells(16HBE) *via* activating Nrf2/GPX4/SLC7A11 pathway. Further studies indicate that the effects of GAA depend on the upregulation of NLRP3. In vivo study suggested that GAA alleviates LPS- induced acute lung injury in mice by inhibiting ferroptosis via upregulating NLRP3 and activating the Nrf2/GPX4/SLC7A11 pathway.

1. Introduction

Acute lung injury (ALI) is a globally recognized respiratory condition characterized by rapid onset, a prolonged course, and a significant threat to patient survival, the mortality rate is as high as 30–60% [1]. The pathological features of ALI are diffuse alveolar damage, severe hypoxemia, and uncontrolled pulmonary inflammation. It can be triggered by a variety of factors, such as bacterial or viral pneumonia, pulmonary hemorrhage, and lung trauma [2]. Despite progress in the clinical treatment of ALI, the mortality rate remains high due to the lack of targeted drug therapies; therefore, there is an urgent need to identify new therapeutic targets and drugs.

Ferroptosis, a recently defined form of regulated cell death driven by iron-dependent lipid peroxidation, has emerged as a critical player in the pathogenesis of various inflammatory diseases, including ALI [3]. Ferroptosis is characterized by the overwhelming accumulation of lipid reactive oxygen species (ROS) due to the failure of antioxidant defenses, particularly the glutathione (GSH)-dependent glutathione peroxidase 4 (GPX4) system [4].Accumulating evidence suggests that the dysregulation of iron metabolism and oxidative stress is intimately linked to the destruction of alveolar epithelial cells during ALI [5]. Targeted inhibition of ferroptosis has also emerged as a new approach for treating ALI.

Ganoderic acid A (GAA), a triterpene compound extracted from the traditional Chinese medicinal herb *Ganoderma lucidum*, has drawn magnificent attention for its potent anti-inflammatory and antioxidant activities [6]. Previous studies have demonstrated that GAA exerts protective effects against inflammatory disorders, including acute pancreatitis and osteoarthritis [7,8]. Given that oxidative stress is a hallmark of both inflammation and ferroptosis, we hypothesized that GAA might possess anti-ferroptotic properties that could be effective treatment for ALI.

The nuclear factor erythroid 2-related factor 2 (Nrf2) signaling pathway is a master regulator of cellular antioxidant responses. Upon activation, Nrf2 upregulates a battery of genes involved in iron metabolism and redox homeostasis, including GPX4 and SLC7A11 [9]. Recent studies suggest crosstalk between Nrf2

and the NLR family pyrin domain containing 3 (NLRP3) inflammasome, although the nature of this interaction in the context of ferroptosis is complex and cell-type dependent [10,11].

In this study, we investigated the therapeutic potential of GAA in lipopolysaccharide (LPS)-induced ALI *in vitro* and *in vivo*. We demonstrate that GAA effectively alleviates inflammation by inhibiting ferroptosis in LPS- induced human bronchial epithelial cells(16HBE), the mechanism involves the activation of Nrf2/GPX4/SLC7A11 pathway. Furthermore, our findings reveal that the protective effects of GAA depend on the upregulation of NLRP3. Altogether, the present study highlights GAA as a promising candidate for the treatment of ALI.

2. Materials and methods

2.1 Cell culture

Human bronchial epithelial cells 16HBE (Huatuo Biotech., Guangzhou, China) were cultured in DMEM medium supplemented with 10% fetal bovine serum and 1% penicillin-streptomycin solution. The culture medium was changed once every 2–3 days. When the cell confluence reached 80%, 16HBE cells were passaged at a ratio of 1: 3 and cultured in an incubator at 37°C with 5% CO_2. The 16HBE cells were treated with different concentrations of LPS (0, 1, 2, 5, 10, 20 μg/ml).

2.2 Detection of ROS and cell viability

The 16HBE cells were collected by centrifuging at 1500 r/min for 5–10 min. The cells were then washed using PBS for 1–2 times, and the pellets were collected by centrifugation. A total of 100 μl of ROS assay stain solution was added to each tube. Finally, after incubation at 37°C for 30 min, 16HBE cells were centrifuged, washed with PBS for 1–3 times, and then resuspended in 200 μl of PBS for the fluorescence detection.

Cell viability of 16HBE cells in each group was detected with CCK8 assay. In brief, cells were seeded in the 96-well plate, after treated with different concentration (10, 20, 40, 80, 160 μM) of GGA for 24 h. 10 μl of CCK8 solution was added, and incubated at 37°C for 1–4 h. The absorbance value at 450 nm was measured with a microplate reader.

2.3 Measurement of ferroptosis biomarkers

Ferroptosis and oxidative stress related biomarkers, such as Fe^{2+}, GSH, GPX4 and MDA were detected using commercial kits following manufacturer's instruction. Fe^{2+} detection kit was purchased from Sigma-Aldrich (USA), GSH, GPX4 and MDA detection kit were obtained from ELK Biotechnology.

2.4 Construction of NLRP3-KO 16HBE cell line

The genomic sequence of *NLRP3* gene was downloaded from the GENE database of NCBI. Guide RNA (sgRNA, AGCATCCTGGCTGTAACATT) was designed using the online website (https://portals.broadinstitute.org/gppx/crispick/public) and the targeting plasmids were constructed.

Each plasmid was then co-transfected into the HEK-293T cells together with pWST-VSVG and pWST-Helper. The lentiviral supernatants were collected after 48 h transfection, which should be used immediately or stored at -80°C. A total of 1 ml of lentiviral supernatants was used to knockout NLRP3 in 16HB3 cells. The supernatant was replaced with complete DMEM medium after infection for 12 h. After lentiviral infection for 30 h, NLRP3 knockout 16HB3 cells were selected using DMEM complete medium containing 2 μg/mL puromycin. After one week of continuous selection, cells were harvested, genomic DNA was extracted, and the sgRNA region was amplified by PCR. Following sequencing verification, cells exhibiting double peaks in the target region, indicating successful editing, were selected for monoclonal culture.

2.5 ELISA assay

The concentration of IL-1β and TNF-α were detected using the IL-1β ELISA kit (Jingmei Biotech., Jiangsu, China) and TNF-α ELISA kit (Jingmei Biotech., Jiangsu, China) according to the manufacturer's instruction. The absorbance was measured at a wavelength of 450 nm using a microplate reader.

2.6 The establishment of mouse ALI model

SPF C57BL/6 mice (6–8 weeks, weighing 20–24 g) were purchased from GemPharmatech Co., Ltd. (Jiangsu, China). Animal experimentation ethics was approved by the Animal Ethics Committee of Chongqing Western Biomedical Technology Co., Ltd. The mice were randomly divided into 5 groups (n = 8/group): Healthy control group, LPS group, LPS + GGA group, LPS+ MCC950 group, and LPS + GGA + MCC950 group. From day 0 to day 17, mice were intragastrically administered with vehicle, GGA, MCC950 and GGA+MCC950. The ALI model was induced by intratracheally injected with LPS (10 μg/kg) 1 h after intragastrically administered on day 17. After the procedure, the mice were placed in an upright position and gently shaken to ensure even distribution of LPS between the left and right lungs. The mice were euthanized 24 hours after LPS administration.

Animal experiments complied with the ARRIVE guidelines and were conducted in accordance with the National Institutes of Health guide for the care and use of Laboratory animals (NIH Publications No. 8023, revised 1978). All surgeries were performed under sodium pentobarbital anesthesia, and every effort was made to minimize the suffering.

2.7 Histological analysis

Mouse lung tissues were fixed in 10% neutral buffered formalin for 24 h, dehydrated, embedded in paraffin, and sectioned (3 μm thick) for histopathological examination. A portion of the tissues was stained with hematoxylin and eosin (H&E) to analyze the pathological changes in lung tissues. The severity of lung injury was evaluated based on interstitial inflammation, neutrophil infiltration, congestion, and edema: 0 indicated mild damage; 1 indicated sub-mild injury; 2 indicated moderate injury; 3 indicated severe damage; and 4 indicated sub-very severe damage. The lung injury score was the sum of individual scores for each category. Another portion of the tissues was subjected to immunohistochemistry (IHC) to assess the inflammatory response and ferroptosis level in mice. The

paraffin-embedded sections were dewaxed in xylene, dehydrated in alcohol, and antigen - retrieval was performed using citrate buffer. The sections were incubated with anti-GPX4 antibody (Cat. No. 67763-1-Ig, 10020795, Proteintech., China) and ati-NLRP3 antibody (Cat. No. DF7438, 87P8121, Affinity, China) overnight at 4°C. Then, the tissue sections were incubated with a horseradish peroxidase (HRP)-conjugated secondary antibody (Beyotime Biotech., China). Finally, the sections were stained with diaminobenzidine (DAB) and counterstained with hematoxylin blue.

2.8 Real-time quantitative PCR

Total RNA was extracted from cells and lung tissues of each group using RNAiso reagent (Cat. No. 9109Q, Takara, Japan). Then, cDNA was synthesized using the Hifair® III 1st Strand cDNA Synthesis Kit (Cat. No. 11139ES10, YEASEN, China) following the manufacturer's instruction. Subsequently, PCR amplification was carried out using the SmartCycler II system (Cepheid Inc., Sunnyvale, CA, USA). GAPDH was used as an internal reference and the relative transcription levels of the target genes were analyzed using the $2^{-\Delta\Delta Ct}$ method. The primer sequences of the qPCR assay are shown in Table 1.

Table 1
The primers for the PCR assay.

Genes			Sequences (5'-3')	Length (bp)
In vitro (human gene)	GAPDH	Forward	AGATCCCTCCAAAATCAAGTGG	130
		Reverse	GGCAGAGATGATGACCCTTTT	
	TNF-α	Forward	CTCCTCACCCACACCATCAG	176
		Reverse	CTGAGTCGGTCACCCTTCTC	
	NLRP3	Forward	AGAAGCTCTGGTTGGTCAGC	113
		Reverse	CAAGGCATTCTCCCCCACAT	
	IL-1β	Forward	AGCTCGCCAGTGAAATGATG	151
		Reverse	TGGTGGTCGGAGATTCGTAG	
	Nrf2	Forward	GATCTGCCAACTACTCCCAGG	125
		Reverse	CGTAGCCGAAGAAACCTCAT	
	GPX4	Forward	CCTCATCGACAAGAACGGCT	89
		Reverse	AGAAATAGTGGGGCAGGTCC	
	SLC7A11	Forward	TCCATGAACGGTGGTGTGTT	114
		Reverse	TGGTAGAGGAGTGTGCTTGC	
In vivo (mouse gene)	GAPDH	Forward	GGTGAAGGTCGGTGTGAACG	233
		Reverse	CTCGCTCCTGGAAGATGGTG	
	TNF-α	Forward	CCACGTCGTAGCAAACCACC	156
		Reverse	CCCTTGAAGAGAACCTGGGAG	
	NLRP3	Forward	GCCCTTGGAGACACAGGACT	192
		Reverse	CACGCACAGATCGCCAAGAT	
	IL-1β	Forward	ATGCCACCTTTTGACAGTGATG	136
		Reverse	TGTGCTGCTGCGAGATTTGA	
	Nrf2	Forward	AAAGCACAGCCAGCACATTC	85
		Reverse	GGGATTCACGCATAGGAGCA	
	GPX4	Forward	CCGTCTGAGCCGCTTACTTA	189
		Reverse	GTGACGATGCACACGAAACC	

Genes			Sequences (5’-3’)	Length (bp)
	SLC7A11	Forward	ACCTGGGCAGGAGAAGGTAGT	192
		Reverse	GACAGGGCTCCAAAAAGTGAC	

2.9 Western blot

Cell or tissues were lysed with cell lysis buffer (Beyotime Biotech., Shanghai, China) for 30 min and then centrifuged at 12000 r/min for 15 min at 4°C. The concentration of protein of each sample was determined using a BCA protein assay kit (TaKaRa, Japan). The protein samples were separated by 8%-12% Bis-Tris PAGE electrophoresis, then, the proteins were transferred onto a polyvinylidene difluoride (PVDF) membrane (Millipore, Bedford, USA). The PVDF membrane was blocked in 5% non-fat milk for 1 h before incubated with specific primary antibodies (1:1000) overnight at 4°C. After washing 3 times with TBST, the PVDF membrane was incubated with the secondary antibody (1: 2000) for 1 h at room temperature. The proteins in PVDF membrane were visualized using an ECL chemiluminescent solution (Applygen Tech., Beijing, China). The quantification of the bands was achieved by densitometry using the Tanon Image system (Tanon, Shanghai, China).

2.10 Statistical analysis

The data were statistically analyzed using GraphPad Prism Version 9 (GraphPad Software, Inc., San Diego, CA, USA). The data was presented as mean ± standard deviation. For data conforming to a normal distribution, paired-sample t-test was used for paired samples, and independent-sample t-test was used for independent samples. One-way ANOVA was used for comparisons among multiple groups. For experimental data that did not conform to normality, the non-parametric Mann-Whitney U test was used. Statistical significance was defined as *$p < 0.05$, **$p < 0.01$, ***$p < 0.001$, and ****$p < 0.0001$.

3. Results

3.1 LPS induced ferroptosis in 16HBE cells

To determine the effective concentration of LPS, 16HBE cells were treated with a series concentration of LPS, and cell viability and reactive oxygen species (ROS) levels were measured. We found that treatment with 10 μg/mL LPS for 24 hours significantly reduced cell viability and induced the production of ROS (Fig. 1A-1B). To clarify whether LPS stimulation is associated with ferroptosis, we further examined ferroptosis-related markers. The results indicated that MDA levels were significantly elevated after LPS stimulation, while GSH content were significant reduced (Fig. 1C-1D). After LPS stimulation for 24 h, the level of Fe^{2+} and ROS was markedly increased when compared the control group (Fig. 1E-1F), while the GPX4 activity was significantly decreased (Fig. 1G). Consistently, the mRNA and protein expression levels of GPX4 and Nrf2 were significantly decreased (Fig. 1H-1J) after LPS stimulation, suggesting that LPS can induce ferroptosis and oxidative stress in 16HBE cells.

3.2 GGA significantly inhibits LPS-induced ferroptosis and inflammation

To investigate the protective effects of GAA, a major bioactive compound in *Ganoderma lucidum*, on LPS-induced 16HBE cells. The results of CCK-8 assays indicated that GAA did not affect the cells viability at the tested concentrations, and pretreatment with GAA significantly reversed the LPS-induced decrease in cell viability (Fig. 2A). GAA effectively reversed LPS-induced increases in MDA levels and GSH depletion (Fig. 2B-2C), and suppressed LPS-induced levels of inflammatory cytokines in supernatant (Fig. 2D-2E). Importantly, GAA significantly reversed the LPS-induced decrease in GPX4 activity (Fig. 2E). Further studies confirmed that GAA significantly upregulated the expression of GPX4, Nrf2, and SLC7A11 at both the gene and protein levels, while downregulating the expression of the inflammatory cytokines TNF and IL-1β (Fig. 2G-2I). These results indicate that GGA effectively inhibits LPS-induced ferroptosis and inflammatory responses *in vitro*.

3.3 Ferroptosis mediates LPS-induced inflammatory responses in 16HBE cells

To determine whether ferroptosis is involved in mediating LPS-induced inflammatory responses, we employed the classic ferroptosis inhibitor Liproxstatin-1 (Lip-1). The results showed that Lip-1 treatment significantly improved LPS-induced decreases in cell viability, reduced MDA concentrations, increased GSH concentrations, and effectively inhibited the release of TNF-α and IL-1β (Fig. 3A-3D). Accordingly, Lip-1 significantly upregulated the gene and protein expression levels of ferroptosis markers GPX4, Nrf2, and SLC7A11, while downregulating the gene and protein expression levels of the inflammatory cytokines TNF-α and IL-1β in 16HBE cells (Fig. 3E-3G). These results obviously demonstrate that ferroptosis is a key event driving the inflammatory response in LPS-stimulated 16HBE cells.

3.4 GGA inhibits ferroptosis by activating NLRP3

The NOD-like receptor purine-binding domain 3 (NLRP3) inflammasome is a protein complex implicated in various inflammation-driven diseases. In general, inhibiting NLRP3 effectively reduces inflammatory responses, thus NLRP3 inhibitors have attracted widespread attention in the scientific community [12]. Contrary to expectations, GAA treatment did not suppress NLRP3 expression; instead, it significantly upregulated both its mRNA and protein levels (Fig. 4A-4C). To verify that GAA exerts its anti-ferroptotic and anti-inflammatory effects by upregulating NLRP3, we generated NLRP3 knockout 16HBE cell line (Fig. 4D-4E). We found that the inhibitory effect of GAA on LPS-induced IL-1β and TNF-α was significantly compromised in NLRP3-KO cells (Fig. 4F-4G). Besides, we found that GAA significantly suppressed the mRNA and protein expression levels of IL-1β and TNF-α and upregulated the mRNA and protein expression levels of GPX4, Nrf2, and SLC7A11 in WT 16HBE cells; however, these effects were markedly attenuated in NLRP3-KO cells. These results strongly suggest that GGA may exert its anti-ferroptotic and anti-inflammatory effects by activating, rather than inhibiting, the NLRP3 inflammasome.

3.5 GGA remarkably ameliorates LPS-induced acute lung injury in mice

To elucidate the effect of GAA in alleviating acute lung injury *in vivo*, we established an LPS-induced ALI model in mice. Hematoxylin and eosin (HE) staining of lung tissue revealed severe destruction of alveolar structures, accompanied by massive inflammatory cell infiltration, hemorrhage, and edema in the LPS-induced ALI model group (Fig. 5A). In contrast, GAA treatment significantly attenuated these pathological changes, alveolar structures were relatively intact, and inflammatory infiltration was markedly reduced (Fig. 5A). Furthermore, GAA treatment significantly reduced the levels of IL-1β and TNF-α in lung tissue (Fig. 5B-5F).

To further investigate the effects of GAA on ferroptosis *in vivo*, we evaluated the ferroptosis-related markers in lung tissue. Consistent with the *in vitro* results, immunohistochemistry (IHC) revealed that the expression of GPX4, Nrf2, and SLC7A11 proteins was downregulated in the lung tissue of the model group when compared to the healthy controls; GAA treatment significantly upregulated the expression of GPX4, Nrf2, and SLC7A11 (Fig. 6A-6C). Further experiment confirmed that GAA can reverse the LPS-induced downregulation of GPX4, Nrf2, and SLC7A11 in lung tissue (Fig. 6D-F). Notably, consistent with *in vitro* findings, GAA treatment also significantly upregulated the gene expression level of NLRP3 protein in lung tissue (Fig. 6G).

3.6 GGA alleviates ALI by upregulating NLRP3

To verify whether GGA exerts its effects in vivo by activating NLRP3, we used the NLRP3-specific inhibitor MCC950. The results showed that MCC950 alone had no significant effect on LPS-induced lung injury, GGA alone notably alleviate the lung injury in ALI model; however, MCC950 significantly compromised the protective effect of GGA against LPS-induced pathological damage lung tissue (Fig. 7A). Additionally, MCC950 compromised the upregulation of ferroptosis-related proteins GPX4, Nrf2, and SLC7A11 mediated by GGA (Fig. 7B-7D). These findings further confirm that GGA exerts its protective effects against ALI by inhibiting ferroptosis through activation of the NLRP3 pathway.

4. Discussion

ALI is a common life-threatening critical condition; despite optimal supportive care, the mortality rate remains as high as 30–60%, its primary etiology being bacterial infection [1]. LPS is an endotoxin secreted by Gram-negative bacteria that acts as an inducer in the classical inflammatory pathway; it induces the release of inflammatory cytokines TNF-α and IL-1β, thereby promoting inflammatory and immune responses [13]. The LPS-induced mouse ALI model is also the most common animal disease model of ALI. In this study, we used LPS-induced 16HBE cells and mice as in vitro and in vivo models, respectively, to investigate the effects of GGA on LPS-induced inflammation and ferroptosis. We found that GGA effectively reduced the level of TNF-α and IL-1β in LPS-induced cells and lung tissue, and notably

alleviated the pathological damage in lung tissue, suggesting that GGA may serve as a potential therapeutic agent for ALI.

Ganoderma lucidum is a traditional Chinese medicinal herb known for its ability to tonify qi, calm the mind, relieve coughing, and alleviate wheezing. It is primarily used to treat restlessness, insomnia, palpitations, coughing and wheezing due to lung deficiency, chronic fatigue with shortness of breath, and loss of appetite. It contains various pharmacologically active components and exhibits multiple pharmacological effects, including anti-inflammatory, antioxidant, and immunomodulatory actions [14]. GGA is one of the crucial pharmacologically active components in *Ganoderma lucidum*. Studies have shown that GGA can attenuate inflammatory responses, scavenge free radicals, and reduce oxidative stress-induced damage [7,8]. ALI is a disease closely associated with inflammation and oxidative stress; thus, GGA's pharmacological activities provide a solid theoretical basis for its application in the treatment of ALI. In the present study, we confirmed that GGA can effectively alleviate ALI in a mouse model, and its effects are closely related to the inhibition of inflammation, oxidative stress, and ferroptosis.

Ferroptosis is a programmed cell death driven by iron-dependent lipid peroxidation, playing a crucial role in oxidative stress and inflammatory responses [15]. Ferroptosis is implicated in exacerbating inflammation and cellular damage; conversely, inhibiting ferroptosis can control inflammatory responses and alleviate disease [16,17]. Previous studies have shown that Fe^{2+} chelators may potentially benefit the alleviation of ALI [18]. In the present study, we found that ferroptosis were observed in LPS-induced *in vitro* and *in vivo* models, whereas GGA effectively reduce LPS-induced ferroptosis, inhibit inflammatory responses, and alleviate ALI, suggesting that the therapeutic effect of GGA on ALI may be related to ferroptosis.

The NLRP3 inflammasome is a multiprotein complex composed of the NLRP3 protein, the ASC protein, and pro-caspase-1 [19]. It is widely believed that NLRP3 activation is closely associated with the pathogenesis of inflammatory diseases. However, recent studies have shown that activation of the NLRP3 inflammasome also plays a protective role by facilitating the clearance of damaged organelles and mitigating cellular damage [20,21]. In this study, we found that GGA can inhibit LPS-induced inflammatory responses both *in vitro* and *in vivo*. However, unexpectedly, GGA treatment led to increased expression of the NLRP3 inflammasome, and knocking out or inhibiting NLRP3 attenuated the anti-inflammatory effects of GGA. Our results reaffirm the protective role of the inflammasome, which appears to be associated with the inhibition of ferroptosis. It has been reported that NLRP3 activation initiates the mitochondrial autophagy pathway [22], and mitochondrial autophagy can inhibit ferroptosis by downregulating mitochondrial ROS [23].

Overall, our study has innovatively demonstrated that GGA exerts anti-inflammatory effects by upregulating the NLRP3 inflammasome to inhibit ferroptosis, thereby offering a potential treatment for

ALI. However, the specific mechanism by which GGA mediates NLRP3-regulated ferroptosis requires further investigation.

Declarations

Ethics approval and consent to participate

This study was approved by Animal Ethics Committee of Chongqing Western Biomedical Technology Co., Ltd. (WST.No20240307C0400630[01]). All procedures were conducted in accordance with the Canadian Council on Animal Care.

Competing interests

The authors declare no competing interests.

Funding

No funding was received for conducting this study.

Author Contribution

YZL and ZY designed the experiments and helped with the revise of manuscript. ZGY generated KO cell lines, performed cellular analyses. YJ performed the animal experiment. LJJ helped with the in vitro and in vivo study. ZL and CXQ were responsible for data analyses and wrote the manuscript.

Data availability

The datasets used and/or analyzed during the current study are available from the corresponding author on reasonable request.

References

1. Tang J, Xu L, Zeng Y, Gong F. Effect of gut microbiota on LPS-induced acute lung injury by regulating the TLR4/NF-kB signaling pathway. Int Immunopharmacol. 2021;91:107272. 10.1016/j.intimp.2020.107272.
2. Liu H, Dong J, Xu C, Ni Y, Ye Z, Sun Z, Fan H, Chen Y. Acute lung injury: pathogenesis and treatment. J Transl Med. 2025;23:926. 10.1186/s12967-025-06994-2.
3. Liu P, Feng Y, Li H, Chen X, Wang G, Xu S, Li Y, Zhao L. Ferrostatin-1 alleviates lipopolysaccharide-induced acute lung injury via inhibiting ferroptosis. Cell Mol Biol Lett. 2020;25:10. 10.1186/s11658-020-00205-0.

4. Bipasha M, Deepali V, Prabal D, Supriya K, Megha B. Ferroptosis: A Mechanism of Cell Death With Potential Scope in Cancer Therapy. Asia Pac J Clin Oncol. 2025;21:465–73. 10.1111/ajco.14172.
5. Yu T, Sun S. Role and mechanism of ferroptosis in acute lung injury. Cell Cycle. 2023;22:2119–29. 10.1080/15384101.2023.2278328.
6. Sui Q, Zhu C, Shi S, Xu J, Zhang J, Wang A, Chen P, Liang G, Zhang Y. Ganoderic acid A: an in-depth review of pharmacological effects and molecular docking analysis. J Ethnopharmacol. 2025;349:119868. 10.1016/j.jep.2025.119868.
7. Zhang L, Wang K, Huang L, Deng B, Chen C, Zhao K, Wang W. Ganoderic Acid A Alleviates Severe Acute Pancreatitis by Modulating Gut Homeostasis and Inhibiting TLR4-NLRP3 Signaling. J Agric Food Chem. 2025;73:1563–79. 10.1021/acs.jafc.4c07635.
8. Liu Y, Zhou C, Tan J, Wu T, Pan C, Liu J, Cheng X. Ganoderic acid A slows osteoarthritis progression by attenuating endoplasmic reticulum stress and blocking NF-Kb pathway. Chem Biol Drug Des. 2024;103:e14382. 10.1111/cbdd.14382.
9. Liu H, Zhang TA, Zhang WY, Huang SR, Hu Y, Sun J. Rhein attenuates cerebral ischemia-reperfusion injury via inhibition of ferroptosis through NRF2/SLC7A11/GPX4 pathway. Exp Neurol. 2023;369:114541. 10.1016/j.expneurol.2023.114541.
10. Hurtado-Navarro L, Angosto-Bazarra D, Pelegrín P, Baroja-Mazo A, Cuevas S. (2022). NLRP3 Inflammasome and Pyroptosis in Liver Pathophysiology: The Emerging Relevance of Nrf2 Inducers. Antioxidants (Basel) *11*. 10.3390/antiox11050870
11. Jain R, Vora L, Nathiya D, Khatri DK. Nrf2-Keap1 Pathway and NLRP3 Inflammasome in Parkinson's Disease: Mechanistic Crosstalk and Therapeutic Implications. Mol Neurobiol. 2025;63:91. 10.1007/s12035-025-05389-0.
12. Chen Y, Ye X, Escames G, Lei W, Zhang X, Li M, Jing T, Yao Y, Qiu Z, Wang Z, et al. The NLRP3 inflammasome: contributions to inflammation-related diseases. Cell Mol Biol Lett. 2023;28:51. 10.1186/s11658-023-00462-9.
13. Facchin BM, Reis D, Vieira GO, Mohr GN, da Rosa ETB, Kretzer JS, Demarchi IF, I.G., and, Dalmarco EM. Inflammatory biomarkers on an LPS-induced RAW 264.7 cell model: a systematic review and meta-analysis. Inflamm Res. 2022;71:741–58. 10.1007/s00011-022-01584-0.
14. Peng H, Zhong L, Cheng L, Chen L, Tong R, Shi J, Bai L. Ganoderma lucidum: Current advancements of characteristic components and experimental progress in anti-liver fibrosis. Front Pharmacol. 2022;13:1094405. 10.3389/fphar.2022.1094405.
15. Yu Y, Yan Y, Niu F, Wang Y, Chen X, Su G, Liu Y, Zhao X, Qian L, Liu P, Xiong Y. Ferroptosis: a cell death connecting oxidative stress, inflammation and cardiovascular diseases. Cell Death Discov. 2021;7:193. 10.1038/s41420-021-00579-w.
16. Zheng D, Liu J, Piao H, Zhu Z, Wei R, Liu K. ROS-triggered endothelial cell death mechanisms: Focus on pyroptosis, parthanatos, and ferroptosis. Front Immunol. 2022;13:1039241. 10.3389/fimmu.2022.1039241.

17. Ma B, Hu X, Ai X, Zhang Y. Research progress of ferroptosis and inflammatory bowel disease. Biometals. 2024;37:1039–62. 10.1007/s10534-024-00604-2.
18. Kostopanagiotou GG, Kalimeris KA, Arkadopoulos NP, Pafiti A, Panagopoulos D, Smyrniotis V, Vlahakos D, Routsi C, Lekka ME, Nakos G. Desferrioxamine attenuates minor lung injury following surgical acute liver failure. Eur Respir J. 2009;33:1429–36. 10.1183/09031936.00123108.
19. Guan Y, Gu Y, Li H, Liang B, Han C, Zhang Y, Liu Q, Wei W, Ma Y. NLRP3 inflammasome activation mechanism and its role in autoimmune liver disease. Acta Biochim Biophys Sin (Shanghai). 2022;54:1577–86. 10.3724/abbs.2022137.
20. Gimenez F, Bhela S, Dogra P, Harvey L, Varanasi SK, Jaggi U, Rouse BT. The inflammasome NLRP3 plays a protective role against a viral immunopathological lesion. J Leukoc Biol. 2016;99:647–57. 10.1189/jlb.3HI0715-321R.
21. Ramachandran R, Manan A, Kim J, Choi S. NLRP3 inflammasome: a key player in the pathogenesis of life-style disorders. Exp Mol Med. 2024;56:1488–500. 10.1038/s12276-024-01261-8.
22. Zhong Z, Umemura A, Sanchez-Lopez E, Liang S, Shalapour S, Wong J, He F, Boassa D, Perkins G, Ali SR, et al. NF-κB Restricts Inflammasome Activation via Elimination of Damaged Mitochondria. Cell. 2016;164:896–910. 10.1016/j.cell.2015.12.057.
23. Yamashita SI, Sugiura Y, Matsuoka Y, Maeda R, Inoue K, Furukawa K, Fukuda T, Chan DC, Kanki T. Mitophagy mediated by BNIP3 and NIX protects against ferroptosis by downregulating mitochondrial reactive oxygen species. Cell Death Differ. 2024;31:651–61. 10.1038/s41418-024-01280-y.

Figures

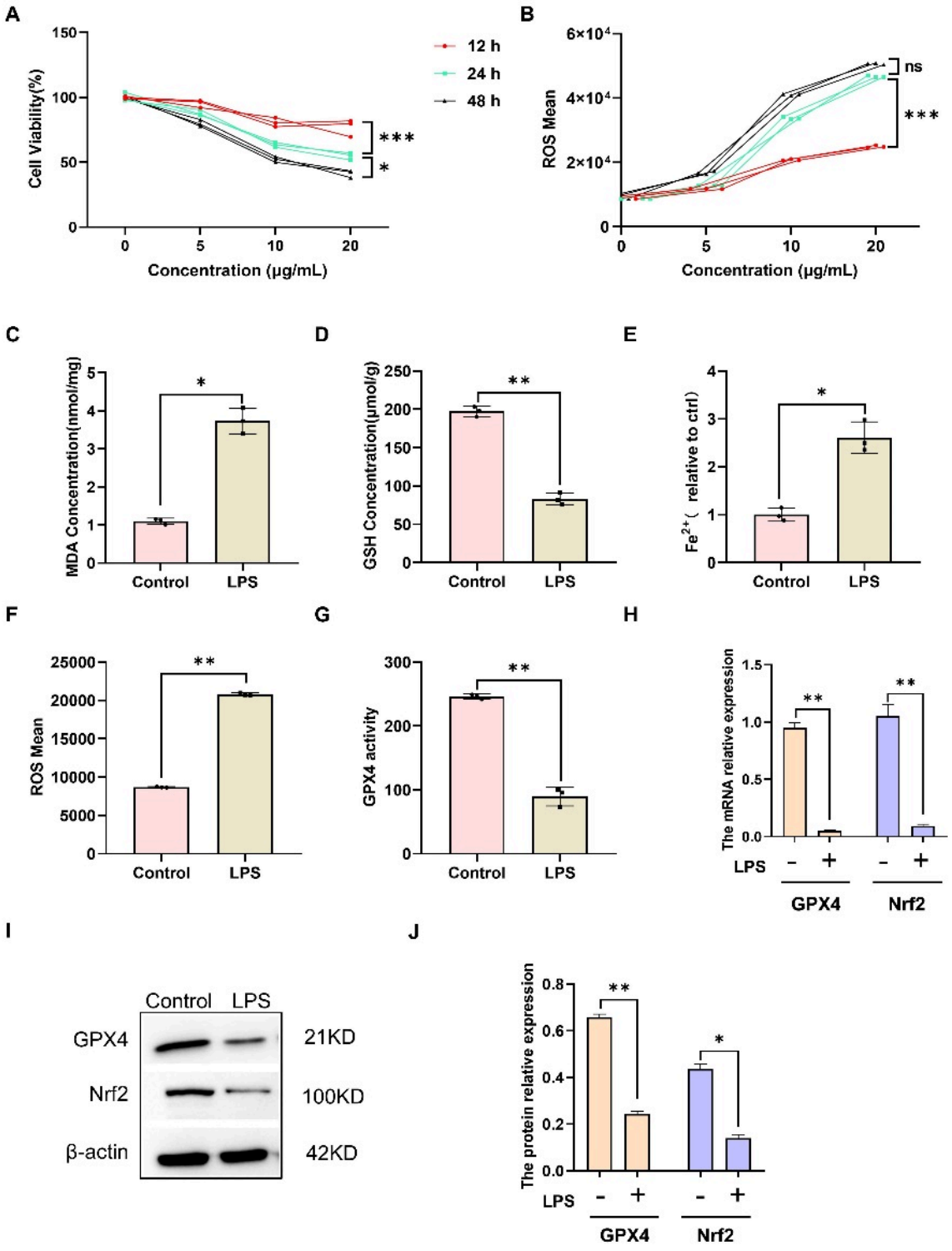


Figure 1

LPS-induced 16HBE cells demonstrated increased levels of ferroptosis. (A) The effect of LPS on 16HBE cell viability; (B) The ROS level induced by different concentration of LPS; (C) The MDA levels induced by LPS; (D) The change of GSH concentration after LPS induction; (E) The change of Fe^{2+} level after LPS induction. (F) The change of ROS level induced by LPS; (G) The activity of GPX4 after LPS induction; (H) The genes expression level of GPX4 and Nrf2 after LPS induction. (I) The protein expression level of

GPX4 and Nrf2 after LPS induction, and (J) the quantitative bar chart. *p<0.05, **p<0.01, ***p<0.001, compared to the control.

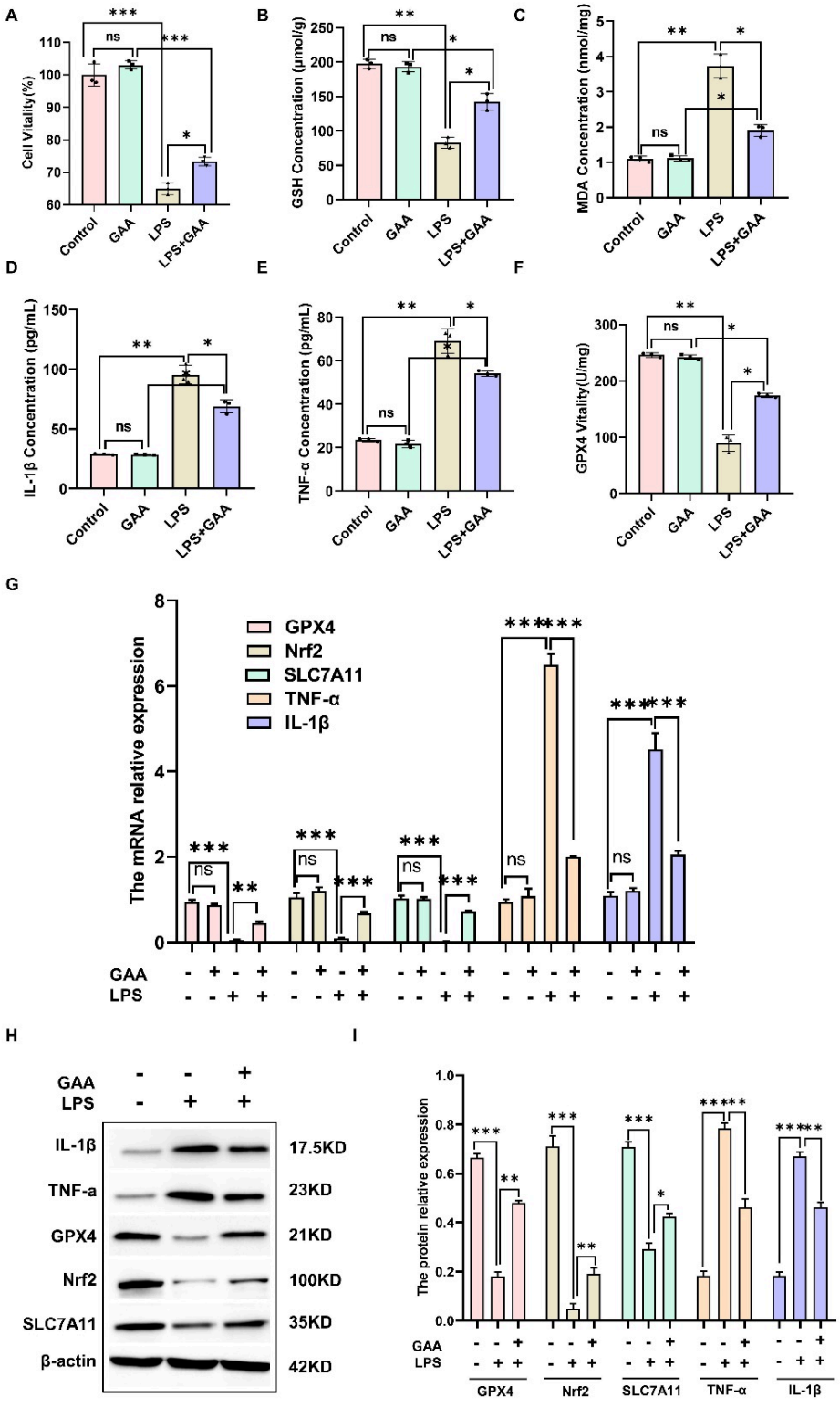


Figure 2

Inhibitory effect of GGA on the LPS-induced ferroptosis and inflammation *in vitro*. (A) The effect of GGA on cell viability after LPS stimulation. The changes of (B) GSH, (C) MDA, (D) IL-1β and (E) TNF-α in LPS-

induced 16HBK cells after GGA treatment. (F) The effect of GGA on GPX4 activity after LPS stimulation. (G) The genes expression level of GPX4, Nrf2, SLC7A11, TNF-α, IL-1β in LPS-stimulated 16HBK cells pretreated with GGA. (H) The protein expression level of GPX4, Nrf2, SLC7A11, TNF-α, IL-1β in LPS-stimulated 16HBK cells pretreated with GGA, and the (I) quantitative bar chart. $^{*}p<0.05$, $^{**}p<0.01$, $^{***}p<0.001$, compared to the LPS induced 16HBK cells.

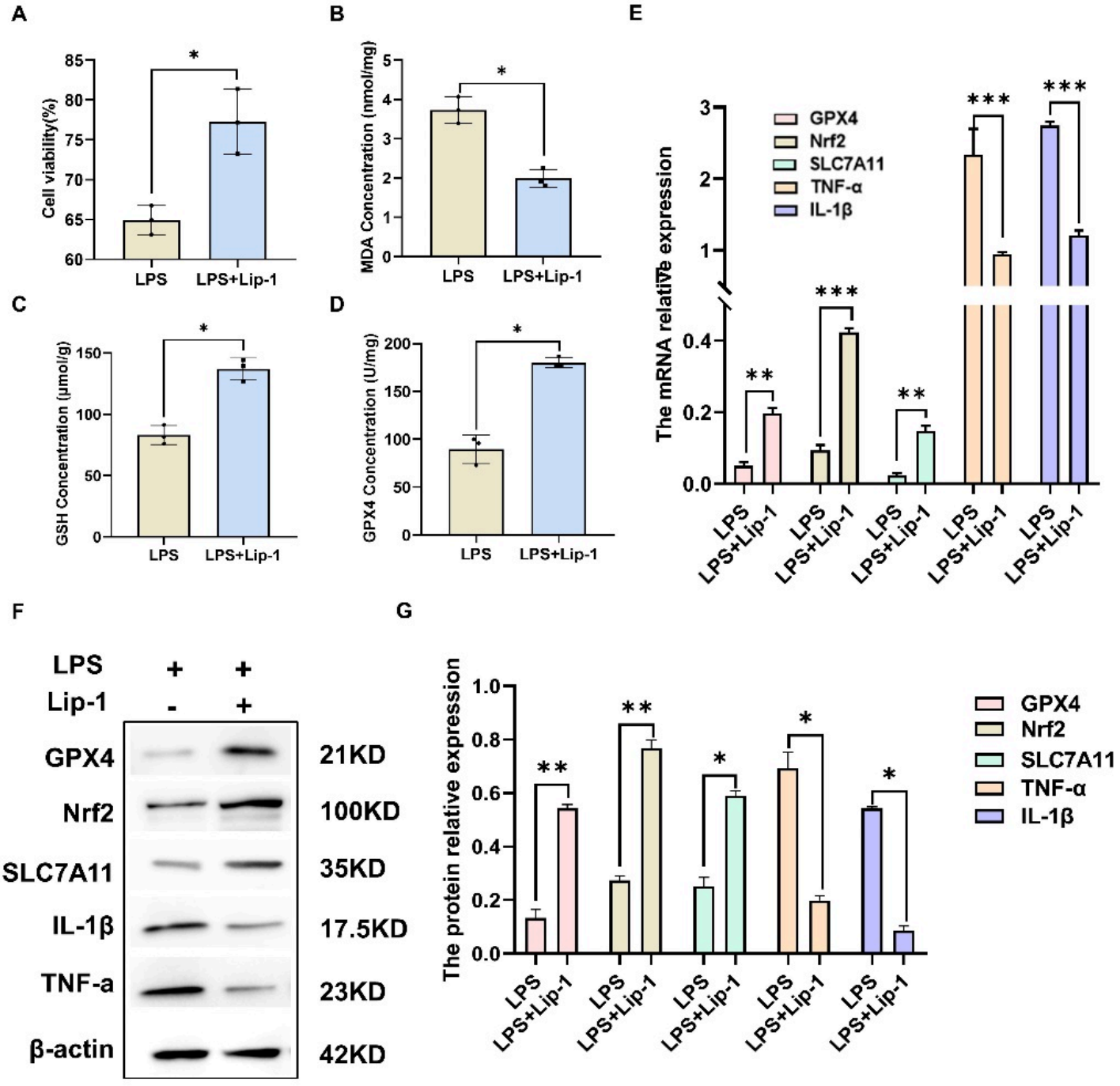


Figure 3

Effects of ferroptosis inhibitor Liproxstain-1 on (A) cell viability, (B) concentrations of MDA, (C) GSH, and (D) GPX4, (E) genes expression level of GPX4, Nrf2, SLC7A11, TNF-α and IL-1β, (F) (G) protein

expressions levels of GPX4, Nrf2, SLC7A11, IL-1β and TNF-α, in the LPS-induced 16HBE cells. *p<0.05, **p<0.01, compared to the LPS-induced 16HBK cells.

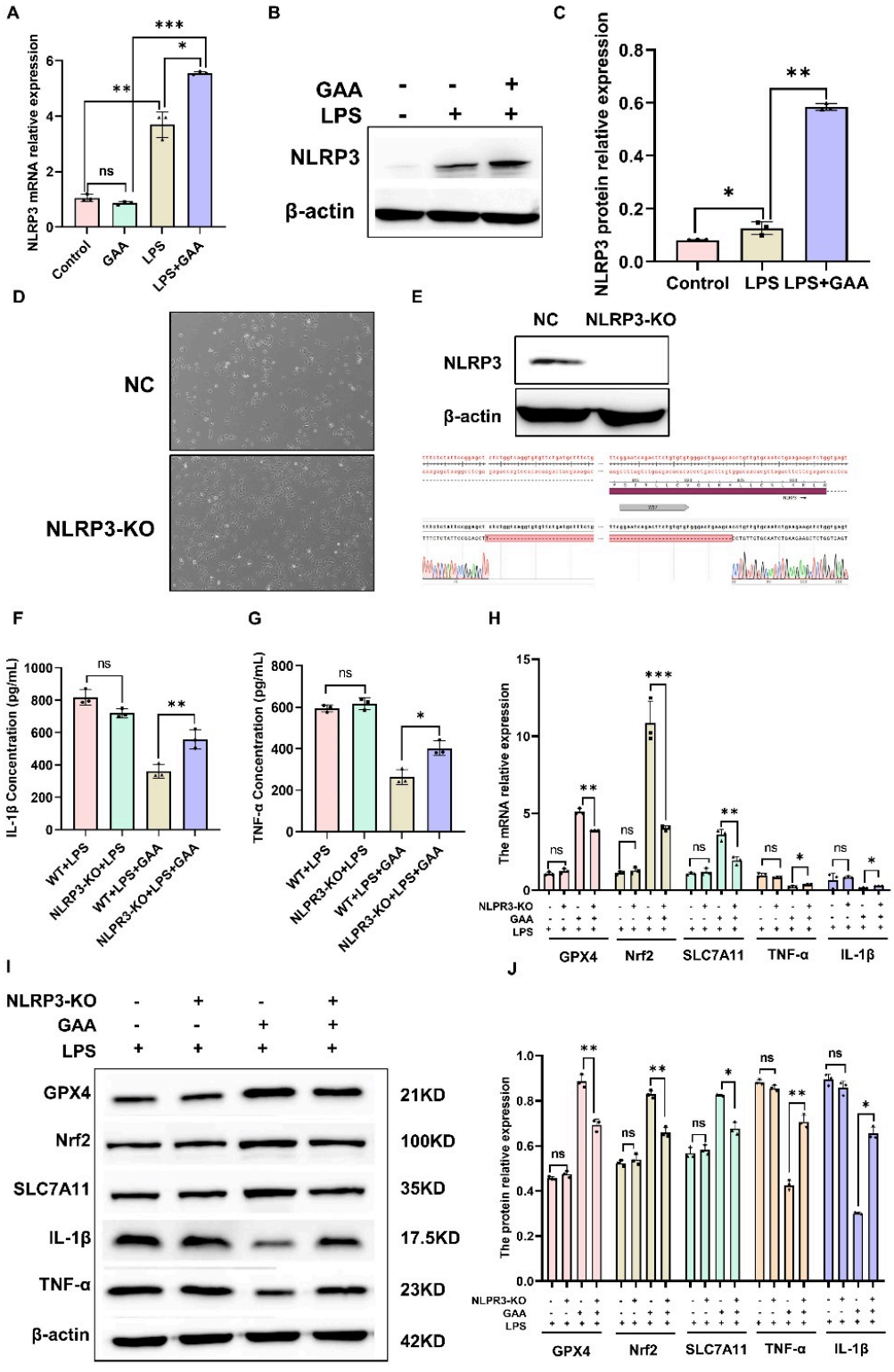


Figure 4

NLRP3 is implicated in the anti- inflammatory and ferroptotic effect of GGA. The (A) gene and (B)(C) protein expression level of NLRP3 in LPS-induced 16HBK cells with GGA treatment. (D) Representative

images following NLRP3 knockout in 16HBK cells (40×). (E) Efficiency of NLRP3 knockout in 16HBK cells. The changes of (F) IL-1β and (G) TNF-α concentration in the supernatant of GGA treated NLRP3 knockout cells with LPS stimulation. The (H) genes and (I) (J) expression level of GPX4, Nrf2, SLC7A11, IL-1β and TNF-α in GGA treated NLRP3 knockout cells with LPS stimulation. $^{*}p<0.05$, $^{**}p<0.01$, compared to the GGA treated WT cells with LPS stimulation.

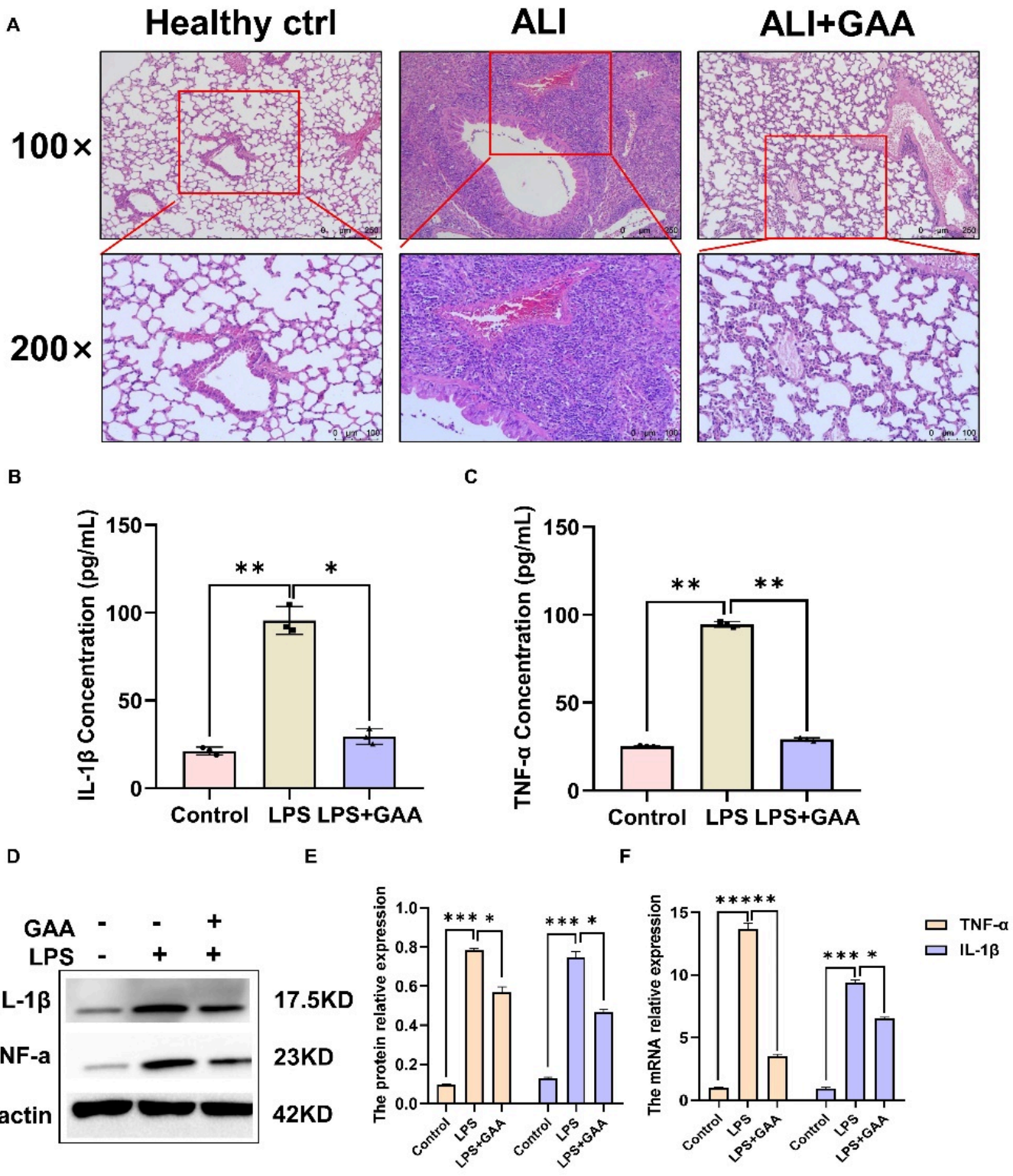


Figure 5

The therapeutic effect of GGA on LPS-induced mouse ALI model. (A) Histopathological changes in GGA treated ALI mice. The concentration of (B) IL-1β and (B) TNF-α in lung tissue supernatant from GGA treated ALI mice. (D) The protein expression levels of IL-1β and TNF-α in lung tissue from GGA treated ALI mice, and the quantitative bar chart. (E) The genes expression level of IL-1β and TNF-α in lung tissue from GGA treated ALI mice. *p<0.05, **p<0.01, compared to the LPS-induced ALI mice model.

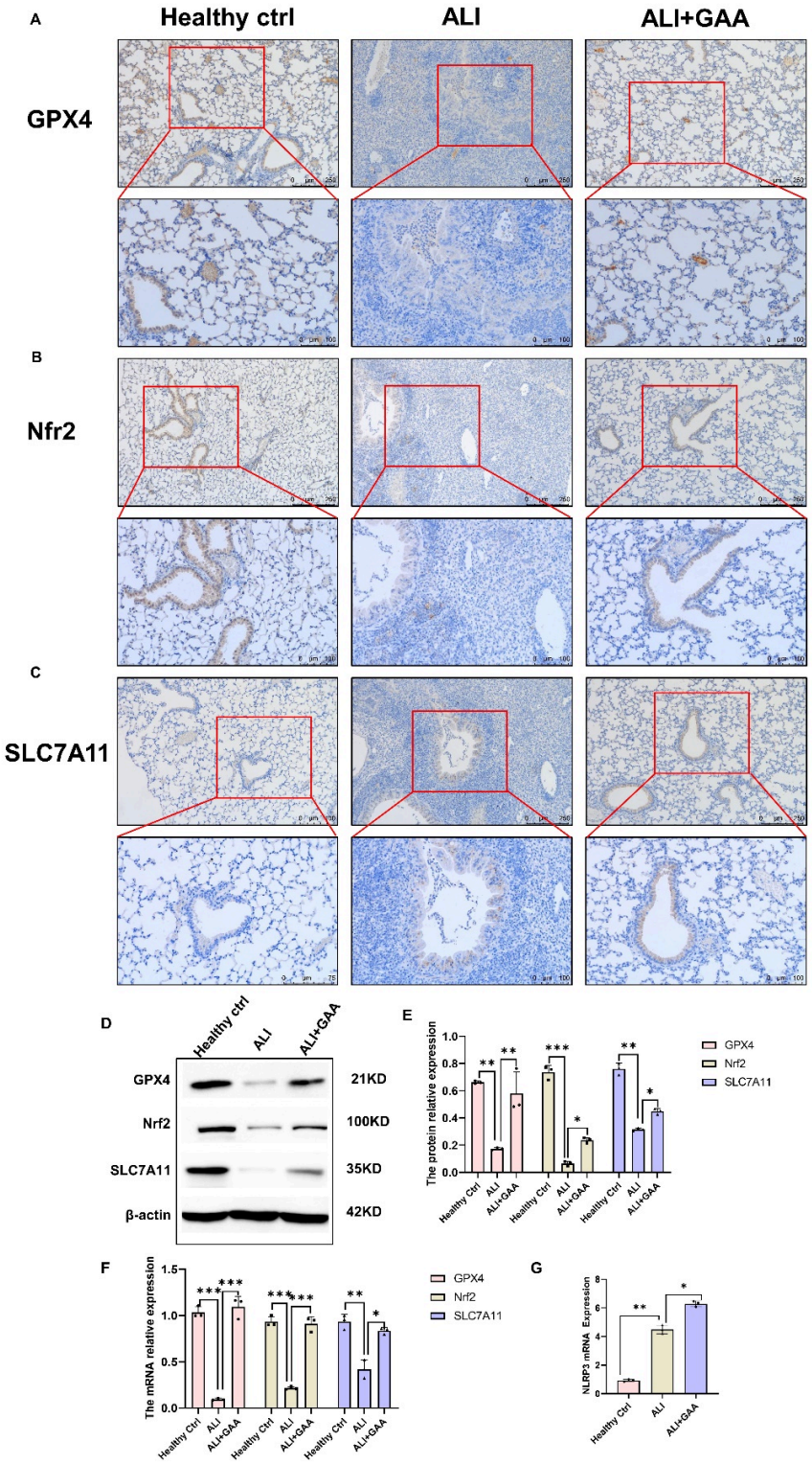


Figure 6

GGA inhibits ferroptosis in LPS-induced ALI mice. Representative immunohistochemical images showing changes in (A) GPX4, (B) Nfr2 and (C) SLC7A11 expression level in mouse lung tissue following GGA treatment. (D) The protein expression level of GPX4, Nrf2 and SLC7A11 in lung tissue from GGA treated ALI mice and the (E) quantitative bar chart. (F) The genes expression level of GPX4, Nrf2 and SLC7A11 in lung tissue from GGA treated ALI mice. (G) The genes expression level of NLRP3 in lung tissue from GGA treated ALI mice.

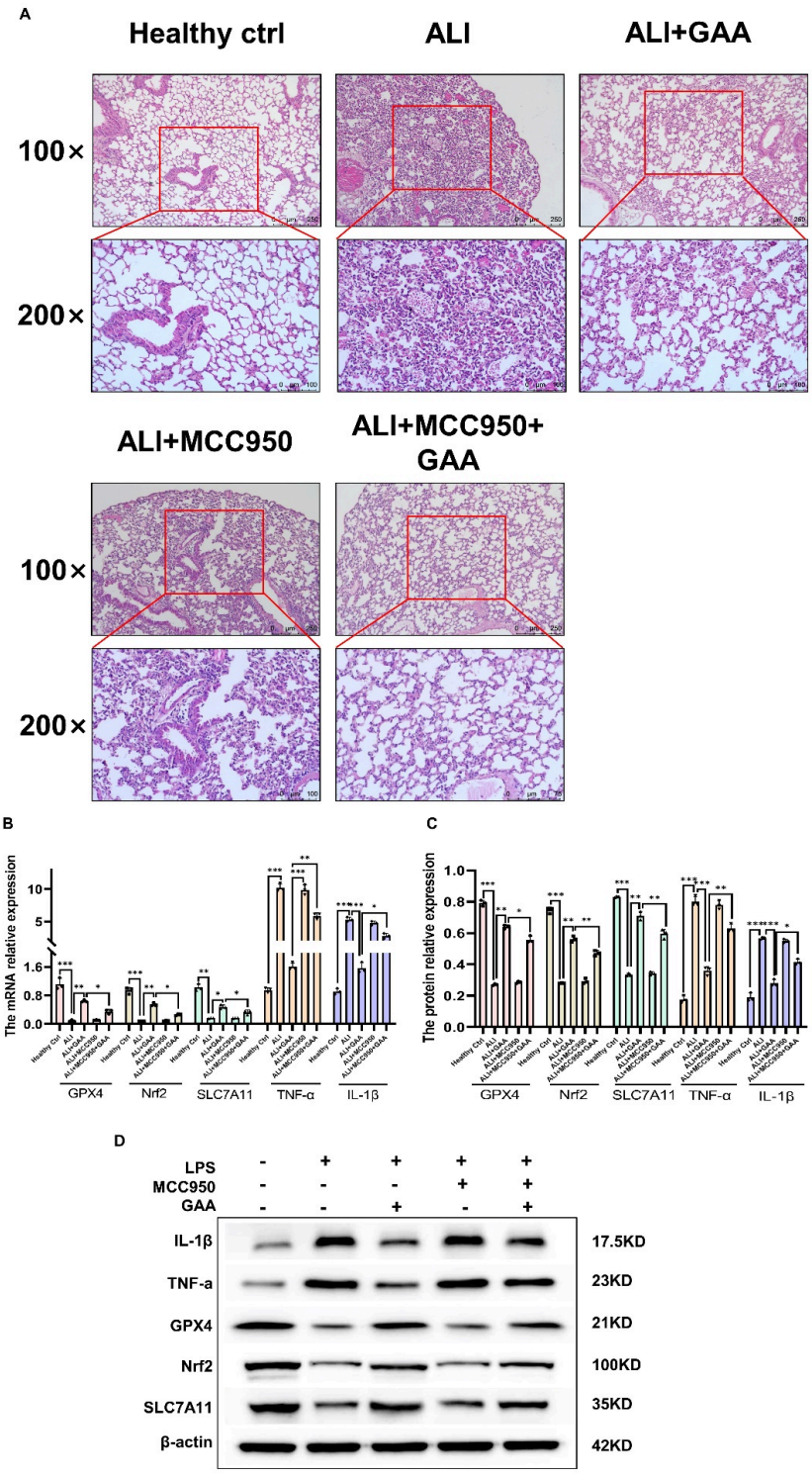


Figure 7

NLRP3 inhibitor, MCC950, compromises the effect of GGA in LPS-induced ALI mice. (A) Histopathological changes in vehicle, GGA, MCC950, GGA plus MC950 treated ALI mice. (B) The genes expression level of GPX4, Nrf2, SCL7A11, TNF-α and IL-1β. (C) (D) The protein expression level of GPX4, Nrf2, SCL7A11, TNF-α and IL-1β.